

Notes

Pyridoxal derived chemosensor: Its application in anion sensing and molecular logic gate building

Suban K Sahoo^{a,*}, Darshna Sharma^a, Shilpa Bothra^a,
Sutapa Mondal Roy^a, Rajender Kumar^a, Ashok Kumar
SK^b, Jitendra P Nandre^c, Umesh D Patil^c & John F Callan^d

^aDepartment of Applied Chemistry, SV National Institute of
Technology (SVNIT), Surat, Gujarat, India
Email: suban_sahoo@rediffmail.com

^bSchool of Advanced Sciences, VIT University, Vellore,
Tamilnadu, India

^cSchool of Chemical Sciences, North Maharashtra University,
Jalgaon, Maharashtra, India

^dSchool of Pharmacy and Pharmaceutical Sciences,
The University of Ulster, Northern Ireland, BT52 1SA

Received 13 November 2015; accepted 31 December 2015

A new chemosensor **L** has been synthesized using Schiff base reaction of pyridoxal with hydrazine and characterized by various spectroscopic techniques such as FTIR, ¹H NMR and mass spectrometry. The anion recognition ability of the synthesized sensor has been investigated by UV-vis, fluorescence and ¹H NMR methods. Among the tested anions, the developed sensor shows a naked-eye detectable color change from colorless to red and spectral changes in the presence of fluoride and acetate ions due to the partial deprotonation of the sensor. With a micromolar detection limit, the developed sensor is highly efficient and may be utilised for the colorimetric detection of fluoride/acetate ions. The developed sensor has been successfully fabricated in to the INHIBIT logic gate at molecular level.

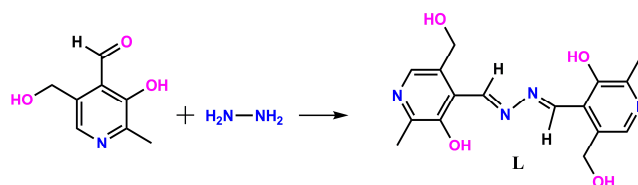
Keywords: Analytical chemistry, Chemosensors, Anion sensors, Fluoride, Acetate, Pyridoxal derivative, Molecular logic gate

Selective anion sensing and recognition is of immense significance due to their wide applications in biomedical and environmental pollution monitoring, anion exchange and anion transport¹⁻⁵. Anions play vital roles in our daily life, being crucial for normal physiochemical functioning of living beings. They play an important role in several industrial processes as well. However, at higher concentrations anions act as harmful pollutant, which makes the development of colorimetric and fluorescent sensors for anion specific sensing, an active area of research¹⁻⁵. The design of the receptors for anion recognition and sensing is a challenging task because of the peculiar characteristics of the anions such as varying size, shape, charge, high hydration energy, and pH-dependent properties.

Nevertheless, significant progress has been made in the development of such sensors, particularly those involving hydrogen-bonding interaction between the anion and receptor component that may be accompanied by deprotonation of an acidic proton on the receptor¹. Among the various bioactive anions, fluoride (F⁻) and acetate (CH₃COO⁻) ions are of particular significance to human health as they are involved in the several important physiochemical phenomena, which make them one of the most attractive sensing targets. Fluoride is added to drinking water to reduce the incidence of dental caries⁶, but at concentrations above the prescribed limits, can give rise to a number of adverse effects such as fluorosis^{7,8}. In particular, high levels of fluoride in drinking water have been associated with both dental and skeletal fluorosis⁹. Because of its high electronegativity, fluoride form strong hydrogen bonds and tend to deprotonate polar –NH or –OH groups. Exploiting the ease with which fluoride ions abstract protons, various optical sensors containing –NH or –OH groups have been developed to detect fluoride and acetate ions¹⁰⁻¹⁴. Similar to fluoride ion, sensing of acetate ion is important due to the role it plays in biology as well as its potential use as a contrast agent in PET imaging¹⁵. Herein, we have introduced a new Schiff base receptor **L**, synthesized by simple condensation of vitamin B6 cofactor pyridoxal and hydrazine (Scheme 1). The anion sensing ability of **L** has been examined by spectroscopic techniques such as UV-vis, fluorescence and ¹H NMR in DMSO and mixed DMSO-H₂O system.

Experimental

The reagents and chemicals used in the present study were purchased from Spectro-Chem Pvt. Ltd.,



Synthesis of the receptor **L** in methanol (refluxed, 2hrs)

Scheme 1

India or Sigma-Aldrich. Solvents such as DMSO and methanol were purchased from Merck, India and were used without any further purification. The anions used for the sensing studies were in the form of their tetrabutylammonium (TBA) salts. The inorganic anions as sodium/potassium salts (NaF, NaAc, $\text{NaH}_2\text{PO}_4 \cdot 2\text{H}_2\text{O}$, KCl and KBr) were purchased from Rankem Pvt. Ltd., India.

All experiments were carried out at 298 K, unless otherwise stated. ^1H NMR spectra were recorded on a Bruker Avance II 400 MHz NMR in $\text{DMSO-}d_6$ using tetramethylsilane (TMS) as an internal standard. The IR spectrum was recorded on a Perkin-Elmer IR spectrophotometer using KBr pellets. The mass spectrum was recorded on a Waters, Q-TOF micromass (LC-MS). Melting point was measured on a digital melting point apparatus VMP-DS "VEEGO" and is uncorrected. UV-vis spectra were recorded on a Varian Cary 50 spectrophotometer in the wavelength range of 200–700 nm with a quartz cuvette (path length = 1 cm at 25 °C) and slit width 2.5 nm. Fluorescence spectra were recorded with a Horiba Fluoromax-4 fluorescence spectrophotometer. For all the spectroscopic experiments, stock solutions (1.0×10^{-4} M) of the sensor **L** and the anions (TBA salts) were prepared in DMSO and stored under a dry atmosphere. These solutions were used for various experiments after appropriate dilutions. For spectroscopic titrations, the required amount of the sensor **L** (2 mL, 1.0×10^{-5} M) was taken directly into cuvette and the spectra were recorded after successive addition of anion solutions.

For the synthesis of **L**, Pyridoxal.HCl (0.5 g, 0.0024 mol) was first desalted by adding KOH (0.13 g, 0.0024 mol) in methanolic medium. Then, hydrazine monohydrate (0.061 g, 0.0012 mol), in 5 mL methanol, was added drop wise at room temperature. The mixture was refluxed for 2 h. A yellow colored precipitate was collected and washed with cold ethanol. The product was recrystallized to form orange crystals and stored in dark. Yield: 87%; M. pt: 210 °C; FT-IR (KBr disc, ν_{max} (cm^{-1}): 3158, 3037, 2841, 1623, 1545, 1403, 1374, 1339, 1292, 1254, 1214, 1070, 1027, 991, 955, 901, 764, 735, 644, 610, 564, 520, 457; ^1H NMR (400 MHz, $\text{DMSO-}d_6$, δ , ppm): 11.75 (1H, s, $-\text{OH}$), 9.38 (1H, s, $-\text{CH}=\text{N}$), 8.03 (1H, s, Ar-H), 5.44 (1H, s, $-\text{CH}_2-\text{OH}$), 4.72 (2H, s, $-\text{CH}_2-\text{OH}$), 2.45 (3H, s, $-\text{CH}_3$); Mass (m/z): Calc. for $\text{C}_{16}\text{H}_{18}\text{N}_4\text{O}_4$: 330; found 331.

Results and discussion

The receptor **L** was synthesized by a Schiff base condensation reaction between the vitamin B6

cofactor pyridoxal and hydrazine (Scheme 1). The ^1H NMR and mass spectra confirm the molecular structure of **L** (Supplementary data, Figs S1-S3). The 3D structure of **L** was optimized at the B3LYP/6-31G** level of theory in the gas phase by applying the computational code Gaussian 09W¹⁶. As shown in Fig. 1, the receptor preferred an enolimine form, stabilized by intramolecular hydrogen bonds. The possible sites for the anion recognition were identified from the Mulliken's atomic charge analysis, which revealed maximum positive atomic charge of 0.313 and 0.340 for $-\text{OH}$ hydrogen of alcohol and phenol followed by the imine (0.125) and methyl (0.127) hydrogen. These sites with maximum positive charge may be the preferred sites of interaction with an incoming anion. The molecular electrostatic potential (MEP) map of **L** (Fig. 1) clearly delineated that the two most positive regions indicated by blue colors are located on the opposite sides around the site of the alcoholic $-\text{OH}$ groups.

The theoretical interpretations were found in confirmation to experimental evidences obtained from

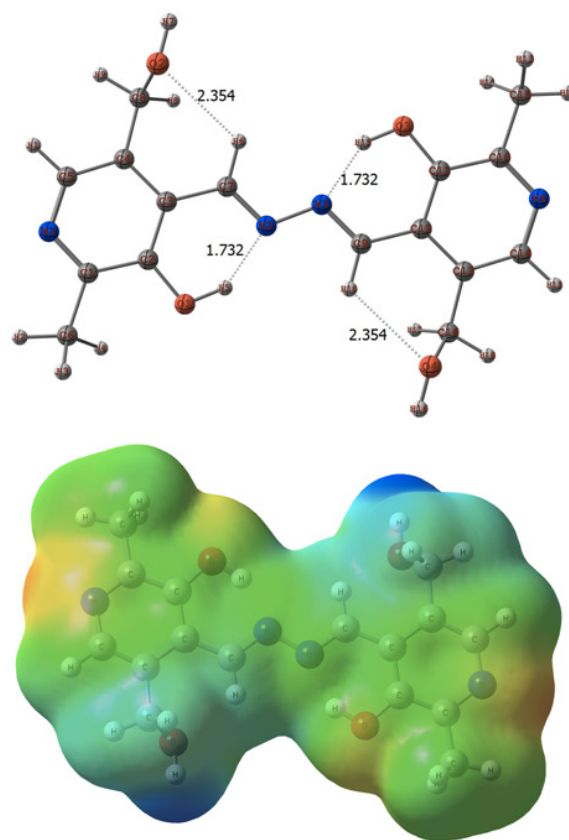


Fig. 1—DFT computed molecular structure of **L** with its MEP diagram (red: negative region, blue: positive region).

UV-visible, fluorescence and naked-eye study of the anion sensing abilities of the receptor **L** towards different anions. The colorimetric sensing ability of **L** ($5.0 \times 10^{-5} M$) with different anions (TBA salts of AcO^- , F^- , Cl^- , Br^- , I^- , HSO_4^- and H_2PO_4^- , $5.0 \times 10^{-4} M$) by naked-eye observation and UV-vis absorption spectroscopy in DMSO is shown in Fig. 2. In the naked-eye experiment, a colorless solution of **L** changed to red immediately on addition of AcO^- and F^- anions. No noticeable color change was observed upon addition of Cl^- , Br^- , I^- and HSO_4^- , except for H_2PO_4^- , which showed a light red coloration. In UV-vis absorption study, the free receptor **L** showed two main absorption bands at 303 nm and 372 nm that were assigned to $\pi \rightarrow \pi^*$ transitions, along with a weak band at 505 nm attributed to a $n \rightarrow \pi^*$ transition. Upon addition of F^- and AcO^- , the band at 372 nm disappeared and the intensity of the band at 303 nm was decreased with significant enhancement in the intensity of the band at 505 nm. The appearance of an intense peak at 505 nm is responsible for the red coloration and is attributed to the formation of receptor-anion complex through intermolecular hydrogen bonding and/or the deprotonation of the $-\text{OH}$ groups of **L**, enabling an internal charge transfer (ICT) between the receptor and the anion. In contrast, trivial changes were observed in the presence of Cl^- , Br^- , I^- , H_2PO_4^- and HSO_4^- anions. Further selectivity study of **L** with other analytes such as NO_3^- , N_3^- , ClO_4^- , benzoate and boronate ions showed

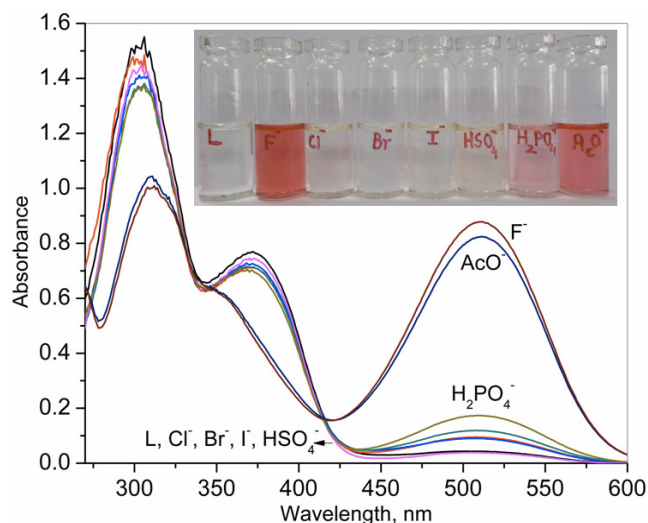


Fig. 2—UV-vis absorption spectra of **L** ($5.0 \times 10^{-5} M$) upon addition of ten equivalents of different anions in DMSO. [Inset: Naked-eye detectable color change of **L**].

no distinguishable color and spectral changes (Supplementary data, Fig. S4). Also, the colorimetric selectivity of **L** towards F^- and AcO^- anions was not affected in the presence of other anions under competitive environment (Supplementary data, Fig. S5).

Upon stepwise addition of the anions (TBAF and TBAAcO) to the solution of **L** ($1.0 \times 10^{-5} M$ in DMSO), both the anions showed similar spectral changes (Fig. 3 and Supplementary data, Fig. S6 with TBAAcO), indicating similar recognition modes during the formation of the new host-guest complex species. With TBAF, the receptor absorption band at 505 nm shows hyperchromic shift and an isobestic point at 420 nm, which supports the formation of a single new component in the solution. Also, the intensity of the receptor band at 303 nm and 372 nm was found to decrease successively. Good linearity was observed in the $0.25 \mu\text{M}$ – $8.47 \mu\text{M}$ range for both TBAF and TBAAcO. The binding constant determined using the Benesi-Hildebrand (B-H) equation¹⁷ revealed that the binding constant for the association of **L** and F^- ($4.81 \times 10^5 M^{-1}$, Supplementary data, Fig. S7) was slightly higher than that for **L** and AcO^- ($3.32 \times 10^5 M^{-1}$, Supplementary data, Fig. S8). The increased affinity of **L** for fluoride may be a result of the shape complementarity between the receptor and the fluoride ion, as well as the higher basicity of this anion compared to AcO^- . Moreover, the B-H plots support the 1:1 binding stoichiometry between the receptor and anions which was complemented using

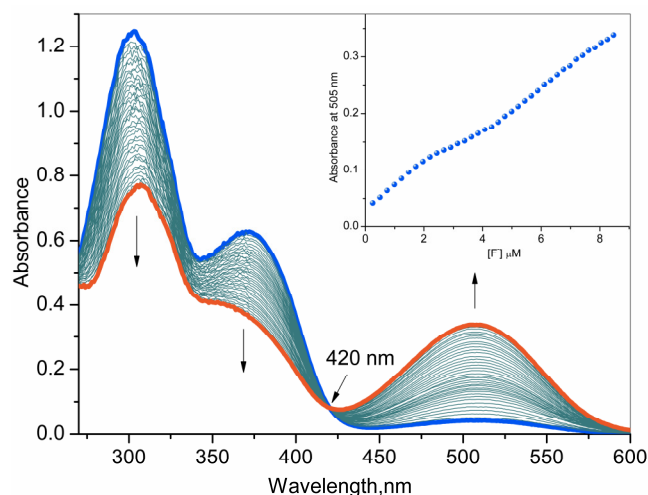


Fig. 3—Changes in the absorption spectrum of **L** ($1.0 \times 10^{-5} M$) upon addition of incremental amounts of TBAF in DMSO.

Job's method of continuous variation (Supplementary data, Fig. S9).

The selectivity of the **L** (5.0×10^{-5} M in DMSO) for anions was also investigated by fluorescence spectroscopy (Fig. 4a). In the free form, **L** showed a weak emission band centred at 640 nm ($\lambda_{\text{exc}} = 510$ nm) that is quenched by the $>\text{C}=\text{N}-$ tautomerism. Upon addition of two equivalents of TBAF and TBAAcO, significant enhancement was observed at 568 nm (blue shifted by 72 nm). The fluorescent enhancement due to TBAF was almost twice that of TBAAcO, indicating a higher affinity of **L** towards fluoride anion. This blue shifted fluorescence enhancement is most likely caused because of prevention of the $>\text{C}=\text{N}-$ isomerization that occurs in the absence of F^- ion, leading to a non-radiative deactivation of the excited state¹³ and also the inhibition of ESIPT upon deprotonation of aromatic-OH protons. No noticeable changes were observed with Cl^- , Br^- , I^- , HSO_4^- and H_2PO_4^- .

The spectra obtained from fluorescence titrations of **L** with incremental addition of TBAF and TBAAcO are shown in Fig. 4b and Fig. S10 (Supplementary data) respectively. Incremental increase in the fluorescence emission intensity was observed at 568 nm upon progressive addition of F^- or AcO^- (0-9 equiv.). Using fluorescence titration data, the detection limit ($3\sigma/S$) of **L** was calculated to be $0.13 \mu\text{M}$ and $1.10 \mu\text{M}$ for F^- and AcO^- , respectively. Moreover, under competitive environment of other anions such as Cl^- , Br^- , I^- , HSO_4^- and H_2PO_4^- ,

negligible interference was observed in the detection of F^- or AcO^- (Supplementary data, Fig. S11).

Apart from the anion sensing ability study of **L**, the anion recognition mode of **L** was also investigated by recording the ^1H NMR spectra of **L** in the absence and presence of different equivalents of TBAF in DMSO- d_6 . As shown in Fig. 5 (see Fig. S12 Supplementary data, for upfield region), the anion free receptor showed a broad singlet at 11.75 ppm corresponding to aromatic -OH protons while the alcoholic-OH protons gave a singlet at 5.44 ppm. The downfield peak due to -OH protons indicates the presence of intramolecular hydrogen bonds as depicted in Fig. 1. The chemical shift for imine, aromatic and methyl protons were observed at 9.38 ppm, 8.03 ppm and 4.72 ppm, respectively. Addition of half equivalent of F^- resulted in the complete disappearance of the aromatic -OH protons signal, whereas the signals due to other protons were shifted upfield. Addition of 3 equivalents of F^- resulted in downfield shift of the alcoholic -OH signal whereas the upfield shift of signals due to imine, aromatic and methyl protons was maintained due to the through-bond effect. No characteristic peak was observed in the region of ~ 16.0 ppm due to the formation of a $\text{F}-\text{H}-\text{F}^-$ complex even after addition of 3 equivalents of fluoride anion¹⁸. Further, the changes in the UV-vis spectra of **L** induced by successive addition of TBAOH was compared with the results obtained in the presence of TBAF and TBAAcO (Fig. 3). The enhancement of absorbance of **L** at 505 nm was half in comparison to fluoride/acetate ions

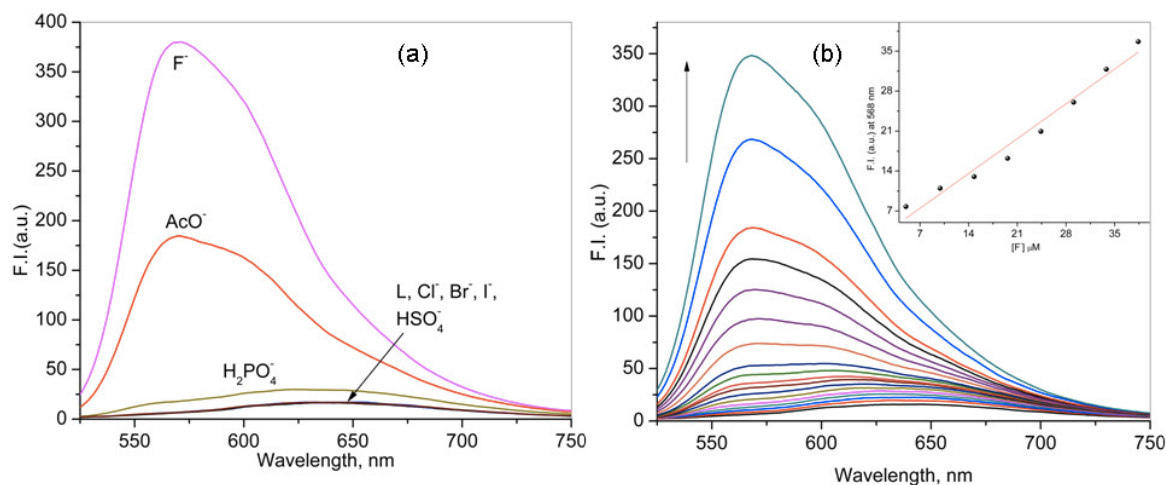


Fig. 4—(a) Changes in the emission spectrum of **L** (5.0×10^{-5} M) on addition of 2 equiv. of different anions and (b) emission titration of **L** (5.0×10^{-5} M) on incremental addition of F^- from $4.98 \mu\text{M}$ to $90.90 \mu\text{M}$ in DMSO. {Inset showing the linear curve fitting of fluorescent intensity at 568 nm as a function of $[\text{F}^-]$ }.

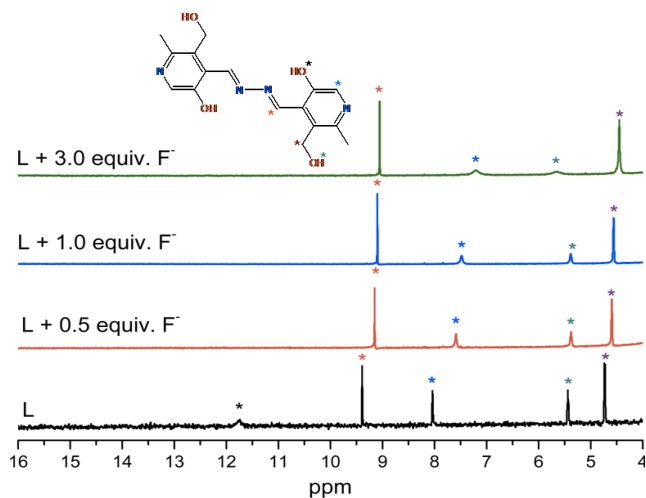


Fig. 5— ^1H NMR spectra of **L** in the absence and presence of different equivalents of TBAF in $\text{DMSO}-d_6$.

under similar conditions (Supplementary data, Fig. S13). These results clearly demonstrated that the anion recognition process by **L** occurred through multiple hydrogen bondings followed by the partial deprotonation of the most acidic aromatic–OH groups of **L** in conformity to the ^1H NMR titration observations¹⁹. In addition, the turn-on fluorescence of **L** with TBAOH in pure DMSO was quenched upon addition of water (Supplementary data, Fig. S14).

The anion selectivity of **L** in $\text{DMSO}/\text{H}_2\text{O}$ (96:4, v/v) system with spiked inorganic (K/Na salts) anions is shown in Fig. 6. The receptor, **L** showed selective colorimetric and spectral changes for the detection of fluoride and acetate anions. Interestingly, the selective ‘turn-on’ response for **L** was also observed in DMSO containing 20% water for both F^- and AcO^- anions (Supplementary data, Fig. S15). In addition, the small optical changes of **L**, observed with H_2PO_4^- in pure DMSO , significantly diminished in the mixed ($\text{DMSO}/\text{H}_2\text{O}$) system.

The sensor **L** has significant practical applications as a colorimetric sensor because of its high ability to form highly red-colored complexes upon binding target anions. To assess the colorimetric application of **L** as a sensor, DMSO solution of **L** (2 mL, 5.0×10^{-5} M) was spiked with different concentrations of NaF or NaAcO (50 μL in H_2O from 1000 μM to 1.0 μM). The naked-eye detection of the anions was observed at as low as 1.0×10^{-5} M (Supplementary data, Figs S16 and S17). The obtained naked-eye detection limit was found to be better than the permissible limit of fluoride ions in drinking water as mandated by United

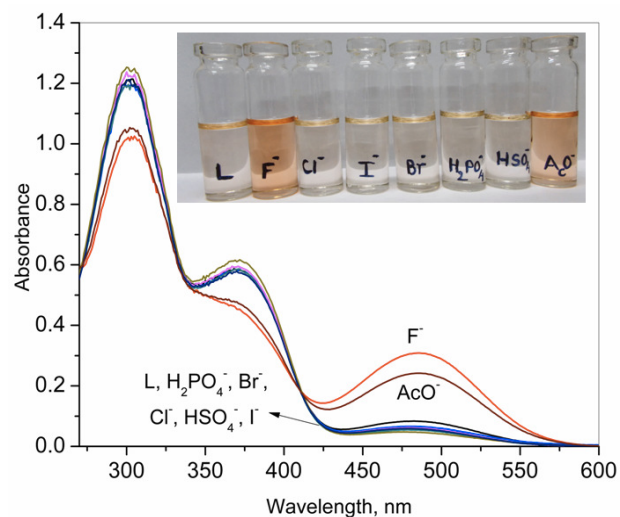


Fig. 6—UV-vis absorption spectra of **L** (5.0×10^{-5} M) in the presence of ten equivalents of different anions in DMSO containing 4% H_2O . [Inset: naked-eye detectable color change of **L**].

States Environmental Protection Agency (USEPA) to prevent osteofluorosis and dental fluorosis²⁰. Further, in the analysis of commercial toothpaste by sensor **L** for the qualitative detection of F^- (Supplementary data, Fig. S18)²¹, a significant red coloration along with an increase in the absorbance band at 505 nm was observed, indicating the successful commercial application of developed sensor. In addition, receptor **L** showed promising sensing ability towards F^- and AcO^- in compared to other reported structurally analogous Schiff base receptors (Supplementary data, Table S1).

Subsequently, the reversibility of **L** (2 mL in DMSO , 5.0×10^{-5} M) was tested for the sensing and discrimination of NaF (50 μL , 1.0×10^{-4} M, in H_2O) and NaAcO (50 μL , 1.0×10^{-4} M in H_2O) by adding CaCl_2 solution (50 μL , 1.0×10^{-3} M in H_2O). As shown in Fig. 7, the color and spectral changes of **L** induced by NaF were reversed in the presence of CaCl_2 . However, in the presence of NaAcO, the receptor color remained intact (Supplementary data, Fig. S19). Thus, **L** can be used for the selective detection of acetate ions in the presence of Ca^{2+} .

Further, this interesting behavior in the different colorimetric states of **L** in the presence of Ca^{2+} and F^- encouraged us to determine the potential of this sensor as a molecular logic gate (Fig. 7). The concept of molecular logics was first reported in 1993 by de Silva *et al.*²². Thereafter, a tremendous amount of

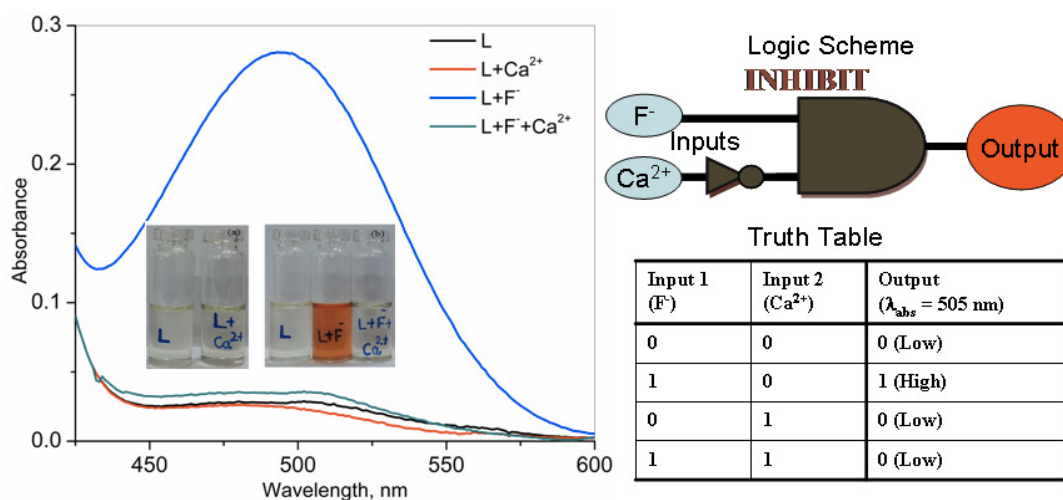


Fig. 7—Construction of molecular logic gate by using UV-vis absorption spectral and color changes of **L** in the presence of Ca²⁺ and F⁻.

effort has been devoted to the fabrication of novel molecular systems capable of performing binary arithmetic and logical operations. In the case of **L**, the visible color change to red or absorbance at 505 nm was taken as an output signal while F⁻ and Ca²⁺ were the two chemical inputs. The absence of (0,0) or the presence of (1,1) both analytes resulted in low absorbance at 505 nm (Supplementary data, Fig. S18). Similarly, the addition of Ca²⁺ alone (0,1) resulted in low absorbance at the output wavelength. However, addition of F⁻ alone (1,0), resulted in a strong absorbance at 505 nm. Based on the above results, the colorimetric or spectral responses of **L** with the two chemical inputs F⁻ and Ca²⁺ satisfies the conditions required for a 2-input INHIBIT molecular logic gate.

In the present study, a simple and easy-to-prepare colorimetric anion sensor **L** was developed using vitamin B6 cofactor. The color of the sensor changed from colorless to red with the introduction of F⁻ and AcO⁻ anions due to the partial deprotonation of aromatic-OH protons. **L** was also found to be selective for F⁻ and AcO⁻ anions in a competitive environment, with a detection limit in the micromolar range. **L** was successfully used for the detection of inorganic fluoride and acetate in aqueous medium and shown to display INHIBIT type molecular logic gate with the inputs of F⁻ and Ca²⁺.

Supplementary data

Supplementary data associated with this article, i.e., Figs S1–S19, and, Table S1, are available in the

electronic form at [http://www.niscair.res.in/jinfo/ijca/IJCA_55A\(01\)44-50_SupplData.pdf](http://www.niscair.res.in/jinfo/ijca/IJCA_55A(01)44-50_SupplData.pdf).

Acknowledgement

This work was made possible by a grant from the Department of Science & Technology, New Delhi, India, (SR/S1/IC-54/2012). SMR sincerely thanks and acknowledges Council of Scientific & Industrial Research, New Delhi, India, for a research associate fellowship and other financial support.

References

- 1 Caltagirone C & Gale P A, *Chem Soc Rev*, 38 (2009) 520.
- 2 Gale P A, *Chem Soc Rev*, 39 (2010) 3746.
- 3 Gale P A, *Chem Comm*, 47 (2011) 82.
- 4 Gale P A, Busschaert N, Haynes C J, Karagiannidis L E & Kirby I L, *Chem Soc Rev*, 43 (2014) 205.
- 5 Wenzel M, Hiscock J R & Gale P A, *Chem Soc Rev*, 41 (2012) 480.
- 6 Featherstone J D, *Comm Dent Oral*, 27 (1999) 31.
- 7 Browne D, Whelton H & O'Mullane D, *J Dent*, 33 (2005) 177.
- 8 Kaminsky L S, Mahoney M C, Leach J, Melius J & Miller M J, *Crit Rev Oral Biol Med*, 1 (1990) 261.
- 9 Schwarzenbach R P, Escher B I, Fenner K, Hofstetter T B, Johnson C A, von Gunten U & Wehrli B, *Science*, 313 (2006) 1072.
- 10 Peng X, Wu Y, Fan J, Tian M & Han K, *J Org Chem*, 70 (2005) 10524.
- 11 Swamy K M, Lee Y J, Lee H N, Chun J, Kim Y, Kim S J & Yoon J, *J Org Chem*, 71 (2006) 8626.
- 12 Sivaraman G & Chellappa D, *J Mater Chem B*, 1 (2013) 5768.
- 13 Sharma D, Sahoo S K, Chaudhary S, Bera R K & Callan J F, *Analyst*, 138 (2013) 3646.
- 14 Sharma D, Ashok Kumar S K & Sahoo S K, *Tetrahedron Lett*, 55 (2014) 927.

- 15 Albrecht S, Buchegger F, Soloviev D, Zaidi H, Veas H, Khan H G, Keller A, Delaloye A B, Ratib O & Miralbell R, *Eur J Nucl Med Mol I*, 34 (2007) 185.
- 16 *Gaussian 09*, (Gaussian, Inc., Wallingford, CT, USA) 2009.
- 17 Benesi H A & Hildebrand J H, *J Am Chem Soc*, 71 (1949) 2703.
- 18 Kumar S S, Bothra S, Sahoo S K & Ashok Kumar S K, *J Fluor Chem*, 164 (2014) 51.
- 19 Sharma D, Mistry A R, Bera R K & Sahoo S K, *Supramol Chem*, 25 (2012) 212.
- 20 Fawell J, Bailey K, Chilton E D J, Fewtrell L & Magara Y, *Fluoride in Drinking Water, WHO Drinking-Water Quality Series*, (IWA Publishing, London, UK, Seattle, USA) 2006.
- 21 Yadav U N, Pant P, Sharma D, Sahoo S K & Shankarling G S, *Sensors Actuators B: Chem*, 197 (2014) 73.
- 22 De Silva A P, Gunaratne H Q N & McCoy C P, *Nature*, 364 (1993) 42.